In-depth approach to fire investigations: microstructural analysis of metallic materials

Marco Boniardi and Andrea Casaroli*,†

Department of Mechanical Engineering, Politecnico di Milano, Via la Masa 1, I-20156, Milan, Italy

1. INTRODUCTION

Research on the cause of what starts a fire and how it develops calls for different techniques, including a visual analysis, which can guide professionals towards a variety of viable alternative solutions [1].

In the case of legal disputes, requirements of rigorous proof based on scientific methods are more and more frequent, which implies that the evidence found at fire sites must be analysed correctly and the data interpreted accurately [2].

For this reason, an analysis of the microstructure is particularly indicated: The metallurgic and microstructural characteristics of the metals and their alloys can be utilized to attain information on the temperatures reached during a fire.

The aim of this report is to clearly demonstrate the potentiality of metallurgic and metallographic analyses of the remains found on fire sites; to show how they can be used, simulations of fires were performed on various components – steel, an aluminium alloy or a copper alloy, which can easily be found on the site of a fire. The various samples obtained were then examined in a laboratory with an optical microscope and a scanning electron microscope (SEM) with energy-dispersive spectroscopy (EDS). The morphologic characteristics and some metallurgic parameters

*Correspondence to: Andrea Casaroli, Department of Mechanical Engineering, Politecnico di Milano, Via la Masa 1, I-20156 Milan, Italy.
†E-mail: andrea.casaroli@polimi.it

Received 7 March 2013; Revised 24 February 2014; Accepted 8 July 2014

that are strictly tied to the thermal actions of the fire (that is, the temperature), such as the state of oxidation, the dimensions of the crystalline grain or the degradation of the edge of the grain of each sample were observed.

Starting from these results, and considering the fact that exposure at different temperatures causes different metallurgic modifications, it is possible to define an interval of temperature the component was exposed to; this fact can be employed to understand how the fire evolved or to validate results obtained by mathematical models, which are increasingly being used in the investigative phase.

2. MATERIAL AND METHODS

Three different metallic components are taken into consideration in this report:

- A cable with three copper conductors in separate insulation (three multistrand conductors).
- Aluminium window frame.
- Carbon steel springs for bed base with steel net.
- Everyday objects that can easily be found in homes that can be subjected to a fire were used; the physical, chemical and/or mechanical properties of the components are standardized by strict regulations (the copper three multistrand conductors) or are not very different from other comparable products available on the market (aluminium window frame and carbon steel springs for bed base with steel net).

All of the components underwent a simulated fire by being heated in a resistance furnace. The thermal parameters imposed on the components included the following:

- Progressive heating until a maintenance temperature was reached.
- Maintaining the temperature for 1 h.
- Air cooling.

At the end of each simulated fire, every component underwent visual analyses, optical microscope analyses and SEM analyses. In the case of the spring, tensile tests were also performed.

2.1. Three multistrand conductors

The three multistrand conductors used as a sample (Figure 1) is a fireproof ethylene propylene rubber-coated wire, whose conductor is made up of Cu-ETP copper (*electrolytic tough pitch* – according to ASTM C11000 or EN CW004A specifications).

Specifications of the chemical composition for this type of material are shown in Table I [3].

The experimental procedure followed for the three multistrand conductors consisted of the following:

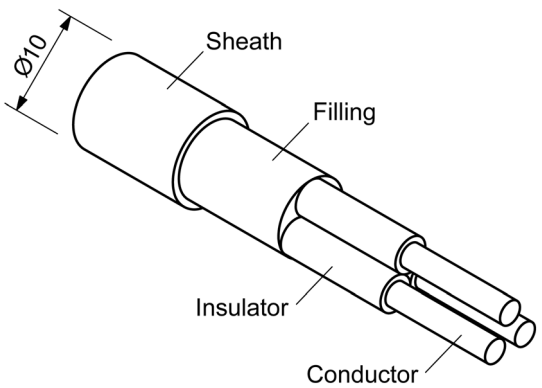

Figure 1. Three multistrand conductors fireproof, ethylene propylene rubber-coated electrical wire with Cu-ETP copper conductors.

Table I. Nominal chemical composition (% weight) of the metallic conductor of the three multistrand conductors.

Cu	O	Pb	Bi
>99.9	>0.005, < 0.04	<0.005	<0.0005

- An initial visual exam and preliminary analyses with an electron microscope (SEM).
- Furnace heating the various pieces of the wire (simulated fire) at the following temperatures: 150, 225, 300, 375, 450, 525, 600, 750 and 900 °C (holding time: 1 h).
- Air cooling to room temperature.
- Visual analysis.
- Preparation and polishing of metallographic samples followed by a chemical attack with a solution of ammonium persulfate (20 g) and distilled water (100 ml) (ASTM 82 attack) [4].
- Optical microscope analysis.

2.2. Aluminium window frame

The aluminium window frame used (Figure 2) was taken from a semifinished, several metre long piece for window casings. It was made up of two separate parts connected by two polyethylene rubber strips. This is an example of a typical type of window frame, whose task is to guarantee thermal insulation by separating the inside from the outside environment.

The chemical analysis performed on the component shows that the window frame is made up of 6060 aluminium alloy, whose chemical composition, according to specifications, can be seen in Table II [3].

The experimental procedure followed for the aluminium window frame consisted of the following:

- An initial visual exam and preliminary analyses with an electron microscope (SEM).
- Furnace heating of the various pieces of the aluminium frame at the following temperatures 150, 225, 300, 375, 450, 525 and 600 °C (holding time: 1 h).

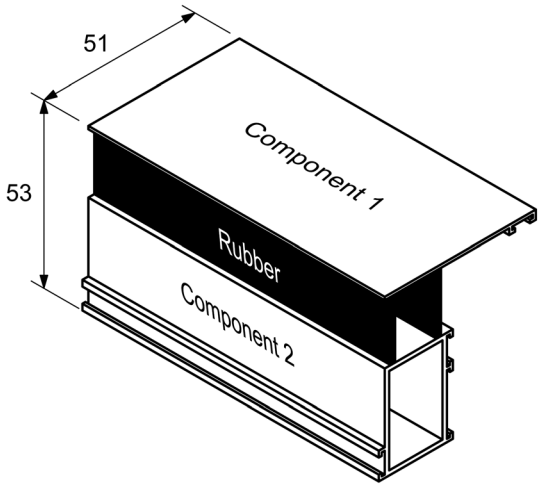

Figure 2. Aluminium 6060 alloy for window frame.

Table II. Chemical composition (% weight) of the aluminium window frame.

Si	Fe	Cu	Mn	Mg	Ti	Zn	Al
0.30 ÷ 0.60	0.10 ÷ 0.30	<0.10	<0.10	0.35 ÷ 0.6	<0.10	<0.15	Bal.

- Air cooling to room temperature.
- Visual analysis.
- Preparation and polishing of the metallographic samples followed by a electrochemical attack with a solution of fluoboric acid (5 ml) and distilled water (200 ml) [4].
- Optical microscope analysis.

2.3. Springs for bed base with steel net

The springs used as samples (Figure 3) were taken from a common bed base with steel net.

The chemical analysis performed on the component indicates that the spring is made up of C60 steel, whose chemical composition, according to specifications, can be seen in Table III [5]. The electron microscope analysis carried out with an EDS probe showed the presence of a zinc surface covering (a zinc-plated spring).

The experimental procedure followed for the analysis of the spring consisted of the following:

- An initial visual exam and preliminary analyses with an electron microscope (SEM).
- Furnace heating of each spring to the following temperatures: 150, 225, 300, 375, 450, 525, 600, 750, 900 and 1050 °C (holding time: 1 h).
- Air cooling to room temperature.
- Visual analysis and SEM analysis (SEM + EDS).
- Preparation and polishing of metallographic samples followed by a chemical attack with a solution of nitric acid (2 ml) and ethanol (100 ml) (2% nital attack) [4].
- Tensile tests.
- Optical microscope analysis.

3. RESULTS AND DISCUSSION

3.1. Three multistrand conductors

3.1.1. Visual analysis. Once taken out of the furnace and air cooled, each piece of the wire was photographed and submitted to a visual analysis of its surface (Figures 4 and 5).

The results are stated as follows:

- 20 °C (control sample): The sheath is light grey; the filling is white; the insulators are yellow/green, blue and brown, whilst the copper of the conductors are bright red.
- 150 °C: There is no alteration of the surface.
- 225 °C: The sheath is soft and has changed shape and colour, becoming light brown, and the insulators do not seem altered.

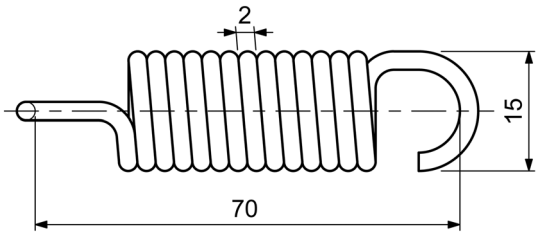

Figure 3. C60 carbon steel spring for bed base with steel net.

Table III. Chemical composition (% weight) of the spring.

C	Si	Mn	S	P	Fe
0.61	0.30	0.75	<0.035	<0.035	Bal.

Figure 4. Visual analysis of the pieces of the heated wire at 20 (control sample), 150, 225, 300, 375 and 450 °C (from left to right).

Figure 5. Visual analysis of the pieces of the heated wire at 525, 600, 750 and 900 °C (from left to right).

- 300 °C: The sheath curls up and is completely charred; the insulators are slightly hardened but not charred.
- 375 °C: The sheath curls up and is completely charred; the insulators are slightly hardened, and some parts are charred.
- 450 °C: Both the sheath and the insulators curl up and catch fire, uncovering the copper wires, which are covered with a layer of grey oxide. The sheath is reddish in some areas. The copper wires are still ductile, and they can be separated by pressing on them slightly.
- 525 °C: No substantial difference from 450 °C.
- 600 °C: No substantial difference from 450 °C.
- 750 °C: The ashes of the sheath lose their red colour and become lighter, except for the area that touches the insulators, which is brownish; the copper wires become more fragile, but it is still possible to separate them by using light pressure.
- 900 °C: The ashes of the sheath are completely brown; the copper wires are quite fragile and cannot be separated without breaking the insulator.

The visual analysis shows how, as the temperature rises, the sheath changes colour progressively, then chars and finally incinerates. The copper tends to be covered by a layer of oxide and becomes more and more fragile (friable to the touch) from 750 °C on.

3.1.2. Optical microscope analysis. After being polished and attacked, each sample was analysed with an optical microscope; the most significant results are shown in Figures 6–9.

The metallographic characteristics, observed at the various sample temperatures are described in the succeeding texts:

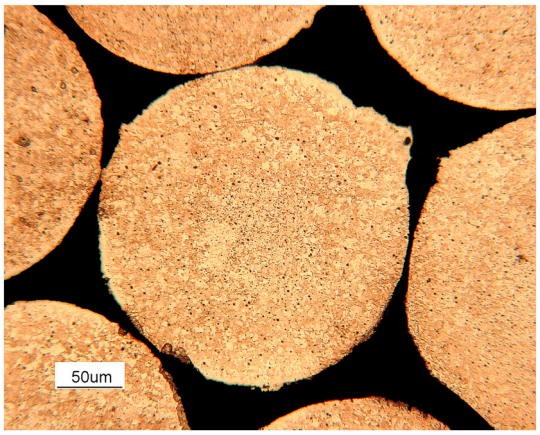

Figure 6. Micrography of the three multistrand conductors at 20 °C (control sample: 200×).

Figure 7. Micrography of the three multistrand conductors heated to 375 °C (200×).

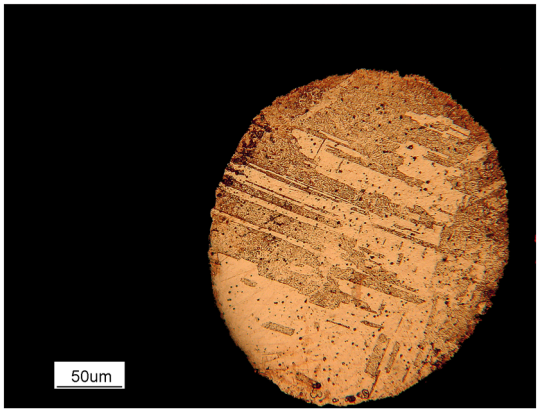

Figure 8. Micrography of the three multistrand conductors heated to 600 °C (200×).

- 20 °C (control sample): Because of the intense hardening during the drawing process, the dimensions of the grains are extremely reduced (approximately from 2 to 8 µm).
- 150 °C: No substantial difference from 20 °C.
- 225 °C: No substantial difference from 20 °C.

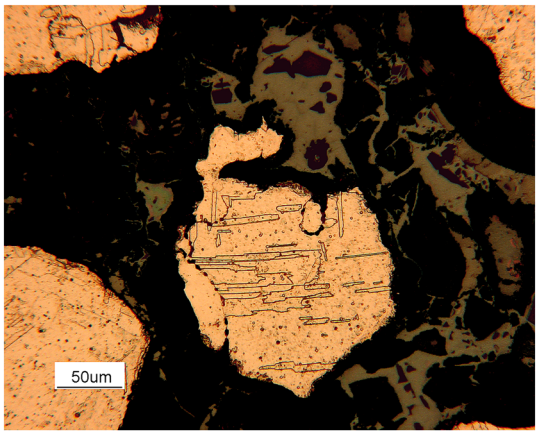

Figure 9. Micrography of the three multistrand conductors heated to 750 °C (200×).

- 300 °C: No substantial difference from 20 °C.
- 375 °C: The crystalline grain has grown, with dimensions from approximately between 25 and 70 µm; this can be attributed to the phenomena of recovery (process by which deformed grains can reduce their stored energy by the removal or rearrangement of defects in their crystal structure) and recrystallization (process by which deformed grains are replaced by a new set of undeformed grains that nucleate and grow until the original grains have been entirely consumed) [6, 7], which is typical of products that have been hardened and subsequently reheated.
- 450 °C: No substantial difference from 375 °C.
- 525 °C: No substantial difference from 375 °C.
- 600 °C: The grain grows further, from approximately between 50 and 150 µm.
- 750 °C: The dimensions of the grain remain similar to those found at 600 °C; there is now a thick layer of oxide around the wires, whose edges are jagged.
- 900 °C: The oxidized area increases; otherwise, there is no significant difference from 750 °C.

The optical microscope analysis demonstrates that, starting from 375 °C, the dimension of the crystalline grain increases, which becomes particularly evident at greater than 600 °C. At 750 °C, a thick layer of oxide forms around the wires, whose perimeter is indistinct and jagged [8, 9].

3.2. Aluminium window frame

3.2.1. Visual analysis. Once taken out of the furnace and air cooled, each piece of the window frame was photographed and submitted to a visual analysis of its surface (Figures 10–12).

Figure 10. Visual analysis of the window frame pieces heated to 20 (control sample), 150 and 225 °C (from left to right).

Figure 11. Visual analysis of the window frame pieces heated to 300, 375 and 450 °C (from left to right).

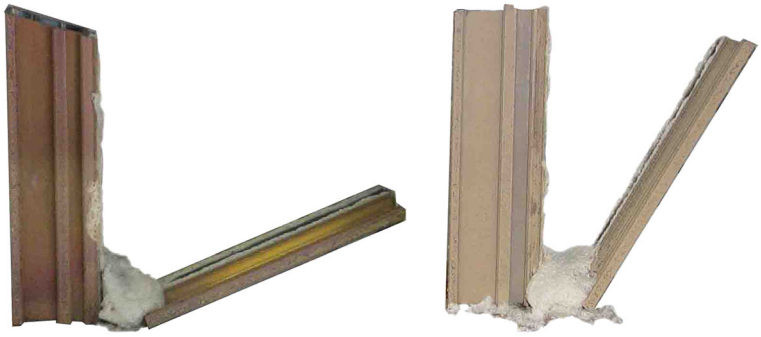

Figure 12. Visual analysis of the window frame pieces heated to 525 and 600 °C (from left to right).

The results are described as follows:

- 20 °C (control sample): The surface is painted to simulate wood and has light and dark brown veins throughout.
- 150 °C: No alterations to the surface.
- 225 °C: The rubber melts, separating the two components. The paint still adheres to the piece but loses its dark brown vein, becoming uniformly light brown.
- 300 °C: The rubber melts, separating the two components. The paint remains adhered to the surface and starts to become dark brown.
- 375 °C: The rubber shows the first signs of charring. The paint remains adhered to the surface and is now dark brown throughout.
- 450 °C: The rubber dilates, exposing some charred areas along with some white or brown spongy zones; both zones crumble easily. The paint pulverizes and again becomes light brown.
- 525 °C: The rubber is completely white and spongy. The paint pulverizes and is light brown.
- 600 °C: No substantial difference from 525 °C.

The visual analysis shows that, as the temperature rises, the rubber first melts, then chars and finally looks spongy. The paint reacts in two different ways:

- Up to 375 °C, it remains adhered to the surface but changes in colour, which goes from homogeneous to light brown and then dark brown.
- Past 450 °C, it pulverizes, separating from the surface, becoming light brown once again.

3.2.2. Optical microscope analysis. After being polished and attacked, each sample was analysed with an optical microscope; the most significant results are shown in Figures 13–15.

The metallographic characteristics observed at the various sample temperatures are described in the succeeding texts:

- 20 °C (control sample): The grains are equiaxed with dimensions ranging approximately from 20 to 60 μm.

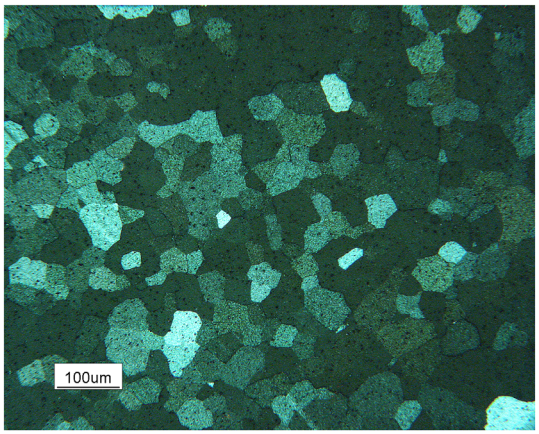

Figure 13. Micrography of the window frame sample at 20 °C (control sample: 100×).

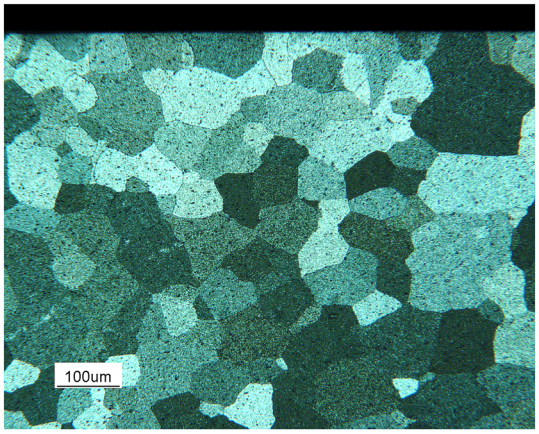

Figure 14. Micrography of the window frame sample heated to 375 °C (100×).

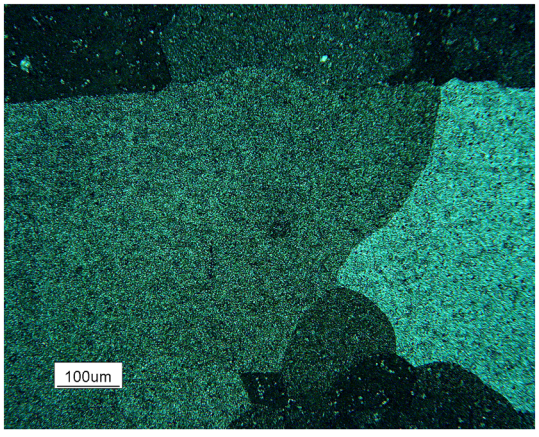

Figure 15. Micrography of the window frame sample heated to 600 °C (100×).

- 150 °C: No substantial difference from 20 °C.
- 225 °C: No substantial difference from 20 °C.
- 300 °C: No substantial difference from 20 °C.

- 375 °C: There is crystalline grain growth in some zones with dimensions in the range approximately 80–200 μm, which can be attributed to the phenomena of recovery and recrystallization.
- 450 °C: No substantial difference from 375 °C.
- 525 °C: No substantial difference from 375 °C.
- 600 °C: There is a further increase of the grain dimensions in some zones, which reaches up to 1000 μm in some areas.

The optical microscope analysis shows a net growth of the crystalline grain dimensions. More precisely, as shown in the following texts:

- From 20 to 150 °C, the dimensions of the grains are approximately from 20 to 60 μm.
- From 375 to 525 °C, some zones of the grain grow, ranging approximately from 80 to 200 μm.
- At 600 °C, some zones of the grain reach approximately 1000 μm.

It is useful to remind that these grain dimensions were reached after an holding time of 1 h; holding times longer than 1 h cause a greater grain growth at the same temperature.

3.3. Springs for bed base with steel net

3.3.1. Visual analysis. After being polished and attacked, each sample was analysed with an optical microscope; the most significant results are shown in Figures 16 and 17.

Figure 16. Visual analysis of the spring heated to 20 (control sample), 150, 225, 300, 375 and 450 °C (from left to right).

Figure 17. Visual analysis of the spring heated to 525, 600, 750, 900 and 1050 °C (from left to right).

The results are reported as follows:

- 20 °C (control sample): The surface is covered with a coat of zinc; it is grey and reflects the light.
- 150 °C: No alterations to the surface.
- 225 °C: No alterations to the surface.
- 300 °C: There are some yellow spots on some of the spring coils.
- 375 °C: The spots expand, covering the entire surface of some of the spring coils.
- 450 °C: The zinc creates a layer of white oxide, which firmly adheres to the surface.
- 525 °C: The zinc oxide layer is firmly adhered to the surface, but some light brown spots appear.
- 600 °C: No substantial difference from 525 °C.
- 750 °C: The oxide layer becomes fragile and turns light grey.
- 900 °C: There are some yellow spots on the zinc oxide layer, and a layer of iron oxide develops beneath it.
- 1050 °C: The zinc oxide layer turns yellow/dark grey; beneath it, the spring develops a layer of iron oxide.

The visual analysis shows that, starting from 450 °C, the zinc on the surface creates a layer of oxide, which initially adheres to the surface and is white in colour; at 750 °C, it becomes fragile and grey/yellow. From 900 °C on, the surface of the spring is completely covered with a layer of iron oxide.

3.3.2. Electron microscope analysis. The electron microscope analysis was performed on three spring coils (from top to bottom: the 2nd – zone 1, the 7th – zone 2 and the 12th – zone 3), comprised both a morphological analysis and a chemical analysis using an EDS probe (Figure 18).

The analysis shows the following (Figures 19–26):

- At 450 °C, the zinc coating oxidizes completely (the surface of the spring coils becomes completely smooth).
- Between 525 and 600 °C, the zinc oxide begins to flake.
- At 750 °C, the zinc oxide becomes fragile and forms flakes that detach from the surface of the spring coils.
- At 900 °C, zinc oxide flakes are stuck between the spring coils, and a layer of iron oxide is beginning to form on the surface, substituting the zinc oxide.
- At 1050 °C, there is no trace of the zinc oxide, and the iron oxide begins to flake (cracks); the layers of oxide that cover the spring coils now adhere to each other.

This behaviour is confirmed by both the morphological analysis and, above all, by the chemical analysis with an EDS probe (Figures 24–26): In fact, between 600 and 1050 °C, that is, when the zinc oxide begins to flake, the percentage of iron increases, and the percentage of zinc decreases.

3.3.3. Optical microscope analysis. After being polished and attacked, each sample was analysed with an optical microscope; the results are shown in Figures 27–31.

The metallographic characteristics, observed at the various sample temperatures, are described in the succeeding texts:

- 20 °C (control sample): Because of drawing, the grains are particularly elongated (major axis: approximately from 10 to 25 μm; minor axis: approximately from 2 to 5 μm).
- 150 °C: No substantial difference from 20 °C.
- 225 °C: No substantial difference from 20 °C.
- 300 °C: No substantial difference from 20 °C.
- 375 °C: No substantial difference from 20 °C.
- 450 °C: No substantial difference from 20 °C.
- 525 °C: No substantial difference from 20 °C.
- 600 °C: No substantial difference from 20 °C.
- 750 °C: Because of the phenomena of recovery and recrystallization [6], the crystalline grain is equiaxed with dimensions ranging from 2 to 10 μm. The structure is pearlitic–ferritic (95% perlite–5% ferrite).

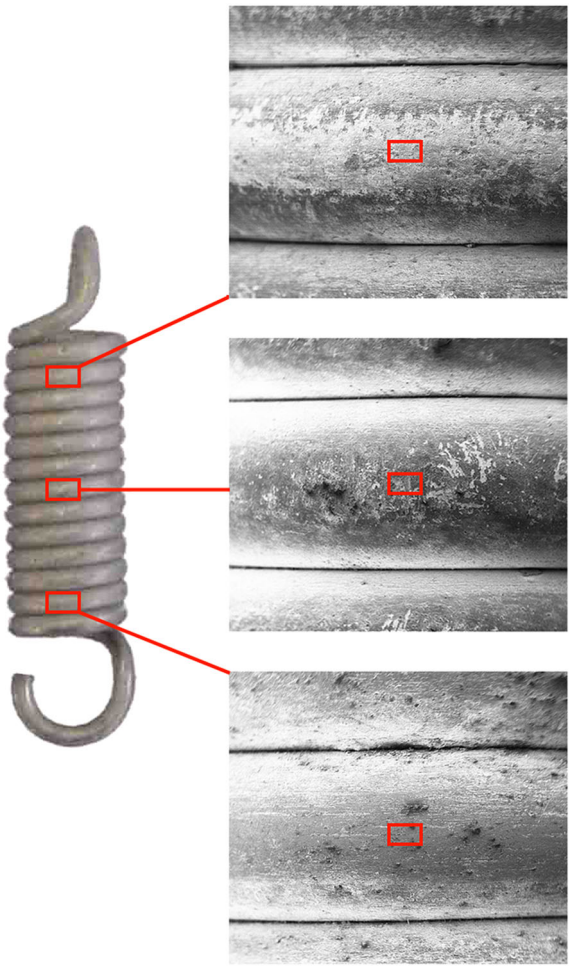

Figure 18. Spring – zones analysed by electron microscope.

Figure 19. Zone 2 – surface of the spring heated to 150 °C (50×).

- 900 °C: The crystalline grain grows, with dimensions ranging from 5 to 20 µm. The crystalline structure is pearlitic–ferritic (90% perlite–10% ferrite).
- 1050 °C: The dimensions of the crystalline grain increase (between 30 and 60 µm). The structure is pearlitic–ferritic (10% pearlite–90% ferrite). The magnification at 200× shows that the

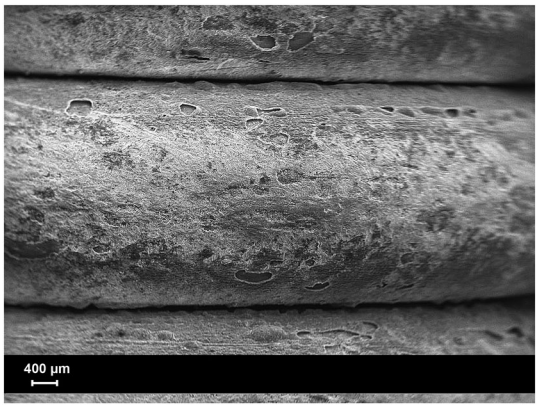

Figure 20. Zone 2 – surface of the spring heated to 525 °C (50×).

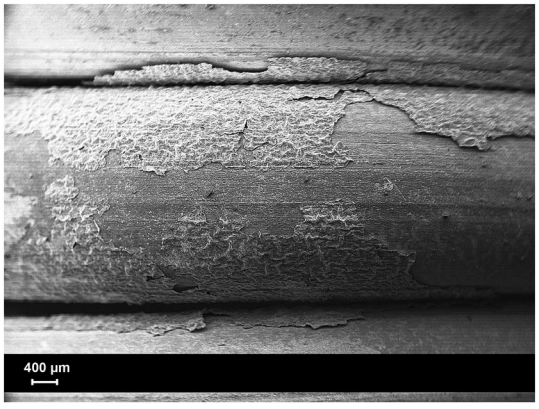

Figure 21. Zone 2 – surface of the spring heated to 750 °C (50×).

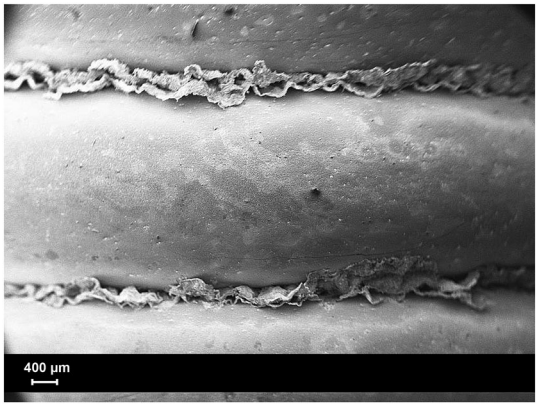

Figure 22. Zone 2 – surface of the spring heated to 900 °C (50×).

spring underwent a substantial superficial decarburizing (a superficial decrease of the carbon content, because of oxidation at high temperature) with a thickness ranging between 50 and 70 µm below the surface.

Figure 23. Zone 2 – surface of the spring heated to 1050 °C (50×).

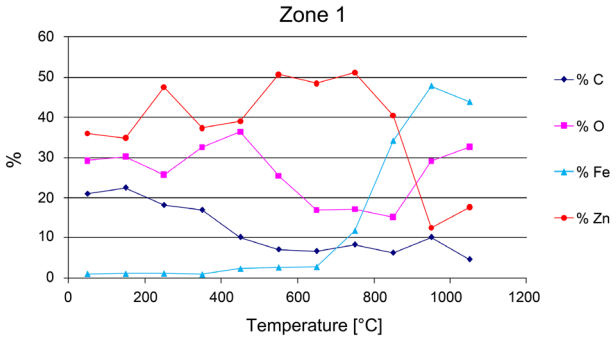

Figure 24. Chemical analysis, using an energy-dispersive spectroscopy probe, of the surface of the spring (zone 1).

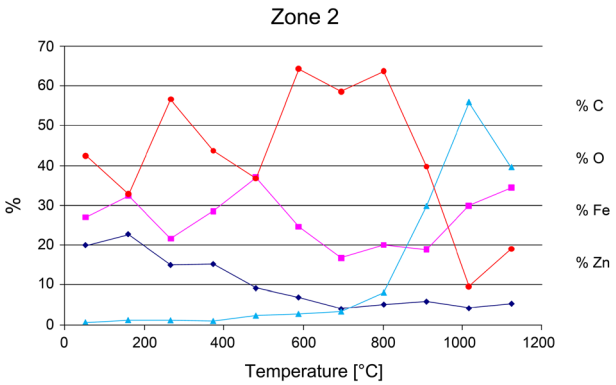

Figure 25. Chemical analysis, using an energy-dispersive spectroscopy probe, of the surface of the spring (zone 2).

The visual analysis shows that, starting from 450 °C, the zinc creates a layer of white oxide that adheres to the surface. Over 750 °C, the oxide becomes fragile, and its colour is e grey/yellow. From 900 °C, even the steel is covered with a layer of oxide.

3.3.4. Tensile tests. Each spring also underwent a tensile test, tracing a strength –elongation diagram for each test. The curves obtained (Figure 32) show how the yield point begins to decrease slightly, starting from 375 °C. The strength curves can be divided into four groups:

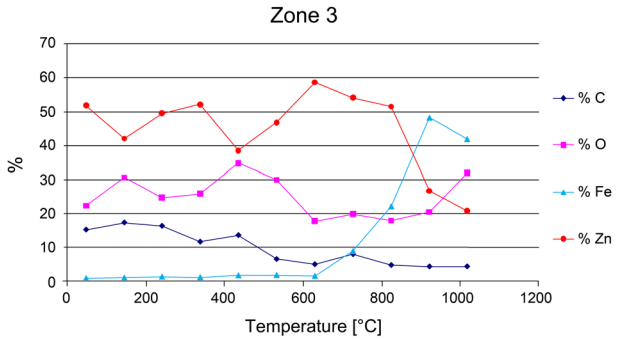

Figure 26. Chemical analysis, using an energy-dispersive spectroscopy probe, of the surface of the spring (zone 3).

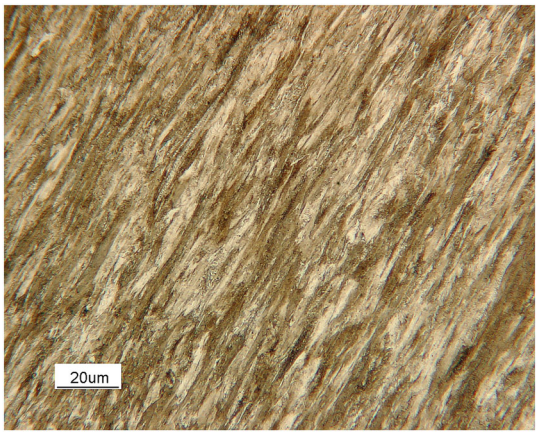

Figure 27. Micrography of the spring sample at 20 °C (control sample: 500×).

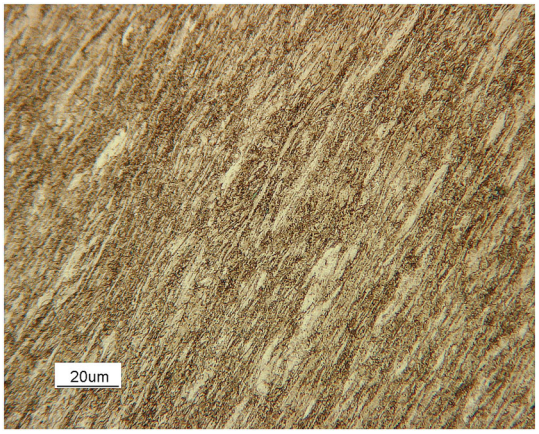

Figure 28. Micrography of the spring sample heated to 600 °C (500×).

- *Group 1* (*spring heated to 300 °C*): The yield point does not suffer from the heating endured during the fire simulation; the spring heated to 225 °C presents a different curve from the others and reaches the breaking point in correspondence to 1080 N and 150 mm of elongation; whereas all the other springs discontinued their tests at 190 mm of elongation without registering signs of weakness or striction of the component.

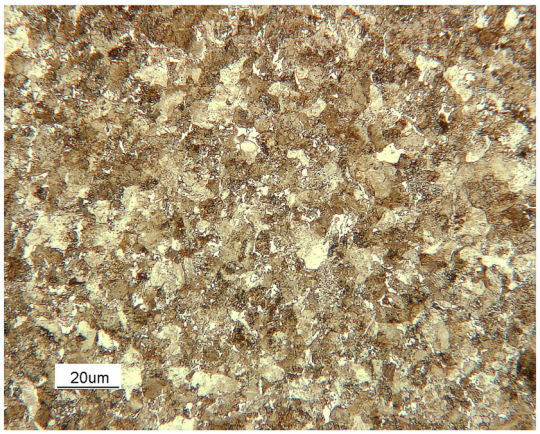

Figure 29. Micrography of the spring sample heated to 750 °C (500×).

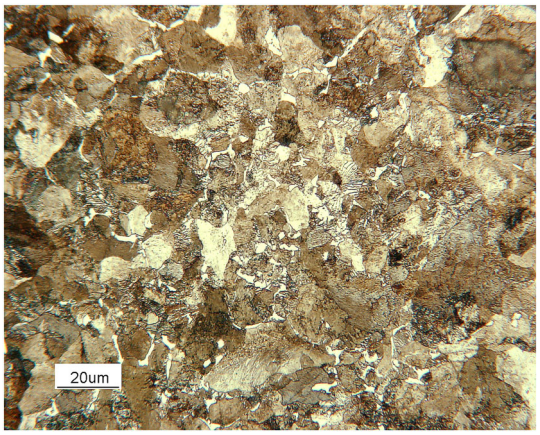

Figure 30. Micrography of the spring sample heated to 900 °C (500×).

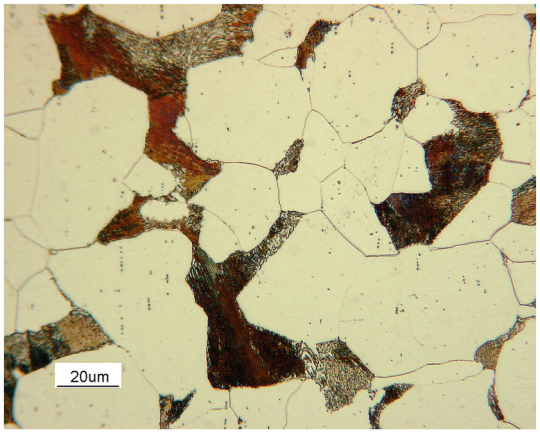

Figure 31. Micrography of the spring sample heated to 1050 °C (500×).

- *Group 2* (*spring heated from 375 to 600 °C*): The yield point decreases slightly as the temperature rises; the form of the strength–elongation curve remains very similar to the one obtained for the springs in group 1 (the plastic stretch is linear and always maintains the same gradient). The test

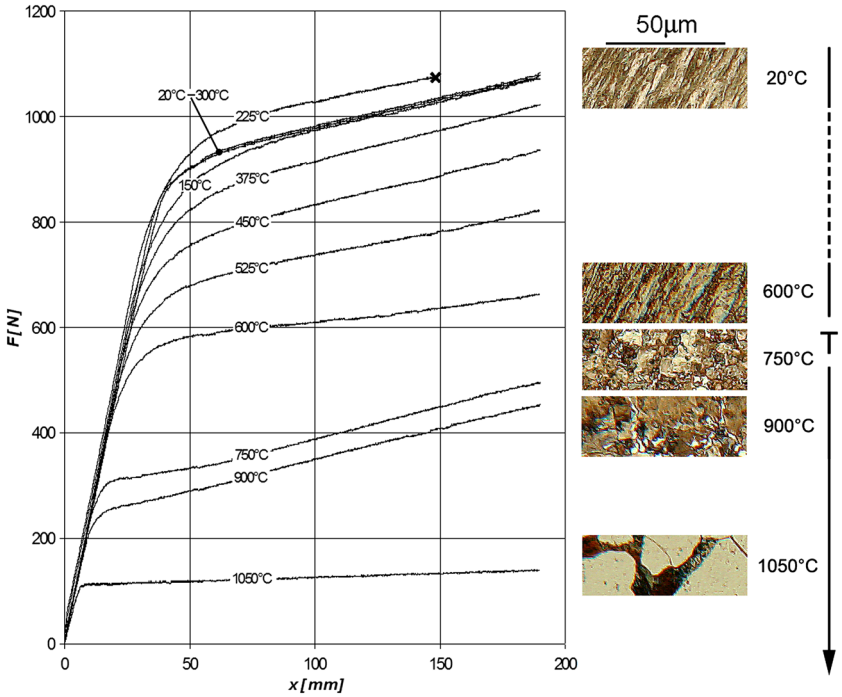

Figure 32. Results of the tests performed for samples heated at various temperatures.

was discontinued for all the springs at 190 mm elongation without registering signs of weakness or striction of the component.

- *Group 3* (*spring heated from 750 to 900 °C*): The yield point is slightly less than that found in group 2, and even the gradient of the plastic stretch is different. The test was discontinued for all the springs at 190 mm elongation without registering signs of weakness or striction of the component.
- *Group 4* (*spring heated to 1050 °C*): The yield point is slightly lower than that of the springs in group 3; the material behaves almost perfectly plastic, with no hardening.

The tensile tests evidenced three interesting elements:

- The yield point of the material decreases starting from 375 °C, which indicates that the *recovery* phenomenon is already active at this point, even if actual recrystallization has not yet begun. This

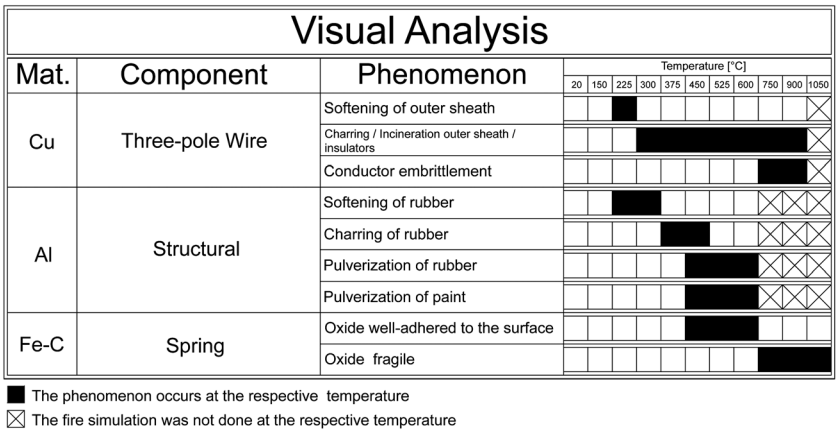

Figure 33. Correlation between temperature and morphological modifications observed on each of the three study samples.

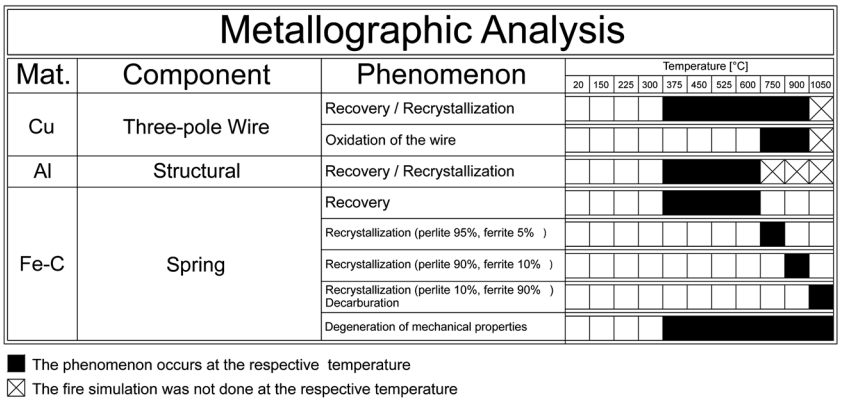

Figure 34. Correlation between temperature and metallurgic modifications observed on all three of the components used in this report.

is why the springs in group 2 (even if their structure is extremely hardened, like the samples in group 1) have much lower yield points. The fact that both groups have the same crystalline structure is confirmed by the micrographics and by the strength–elongation curves, which highlight the same gradient in the plastic section.

- The drastic decrease of the yield point and the change of the gradient in the plastic phase of the springs in group 3 verify that, at temperatures between 750 and 900 °C, recrystallization of the steel occurs, passing from an extremely hardened structure to a structure that is pearlitic–ferric equiaxed. The drastic decrease of the yield point and the almost perfect plasticity of the springs in group 4 verify that, at these temperatures, their microstructure is almost entirely ferric.

4. CONCLUSIONS

Three common components are presented in this report (three multistrand conductors, window frame and springs for bed base with steel net), which are easily found where a domestic fire might occur. Each component underwent simulated fire, exposing them to various temperatures. The three components were analysed using common metallurgic tests (morphologic observation, optical microscope analysis, SEM analysis and tensile tests) to associate one or more morphological–microstructural alterations at each temperature on the component.

The results obtained highlight how some specific morphologic or microstructural alterations (oxidation, recovery, recrystallization, grain growth, etc.) can be useful in determining the maximum temperatures reached by these components, similar to the tests already performed on nonmetallic materials [10].

In the wake of these results, discussed in the previous paragraphs, it is, therefore, possible to acquire tables that highlight the more important morphological and microstructural alterations by correlating their appearance to a given temperature (Figures 33 and 34).

Consequently, the discovery of these components at the site of a fire could be of valuable help in determining the maximum temperatures reached during the fire.

However, some cautionary words are called for in moving from laboratory conditions to the real world. It is important to remember that all the tested specimens have a small thickness, they have a homogeneous temperature throughout the thickness and they were cooled in air. For these reasons, it is meaningful to entrust to an expert judgement in addition to referring to Figures 33 and 34.

REFERENCES

1. NFPA 921. Guide for Fire and Explosion Investigations. National Fire Protection Association (NFPA): Quincy, Massachusetts, 2008.
2. Lentini JJ. Scientific Protocols for Fire Investigation. CRC Press: Boca Raton, Florida, 2006.

3. ASM Handbook, Volume 2, Properties and Selection: Nonferrous Alloys and Special-purpose Materials. ASM International: Materials Park, Ohio, 2004.
4. ASM Handbook, Volume 9, Metallography and Microstructure. ASM International: Materials Park, Ohio, 2004.
5. Callister WD. Material Science and Engineering: An Introduction (5th edn). Wiley: New York, 2000.
6. Askeland DR. The Science and Engineering of Materials (5th edn). Thomson: Cheltenham, UK, 2007.
7. Levinson DW. Copper Metallurgy as a Diagnostic Tool for Analysis of the Origin of Building Fires. *Fire Technology* 1977; **13**:211–222.
8. Babrauskas V. Fires due to electric arcing: can 'cause' beads be distinguished from 'victim' beads by physical or chemical testing? *Fire and Materials* 2003; Conference Proceedings: 189–201.
9. Seki T, Hasegawa H, Imada S, Isao Y. Determination Between Primary and Secondary Molten Marks on Electric Wires by DAS. National Institute of Testing and Evaluation: Kiryu, Gunma, 2000.
10. Babrauskas V. Charring rate of wood as a tool for fire investigations. *Fire safety Journal* 2005; **40**:528–554.